Interface engineering through atomic dopants in HfO_2-based gate stacks

H. Zhu, Ganpati Ramanath, and R. Ramprasad

Citation: Journal of Applied Physics **114**, 114310 (2013); doi: 10.1063/1.4821797
View online: https://doi.org/10.1063/1.4821797
View Table of Contents: http://aip.scitation.org/toc/jap/114/11
Published by the American Institute of Physics

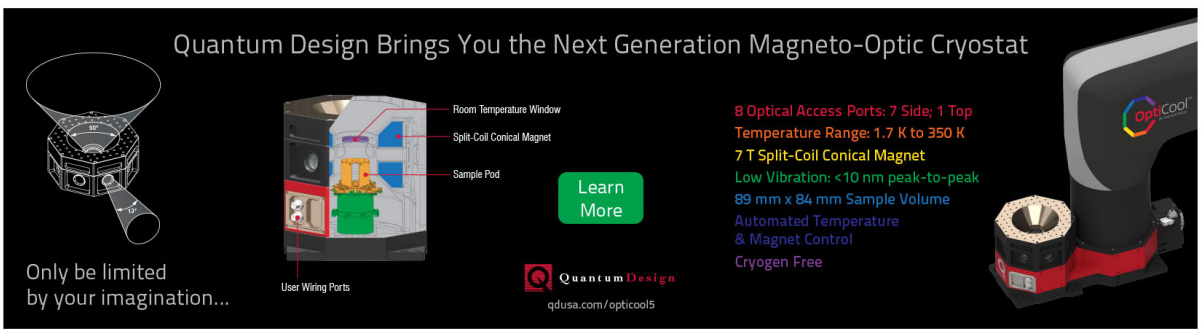

Interface engineering through atomic dopants in HfO_2-based gate stacks

H. Zhu,[1] Ganpati Ramanath,[2] and R. Ramprasad[3]
[1]*Department of Materials Science and Engineering, Massachusetts Institute of Technology, 77 Massachusetts Avenue, Cambridge, Massachusetts 02139, USA*
[2]*Department of Materials Science and Engineering, Rensselaer Polytechnic Institute, Troy, New York 12180, USA*
[3]*Department of Materials Science and Engineering, and Institute of Materials Science, University of Connecticut, 97 North Eagleville Road, Storrs, Connecticut 06269, USA*

(Received 23 August 2013; accepted 3 September 2013; published online 19 September 2013)

Controlling the effective work function (ϕ_{eff}) of metal electrodes is critical and challenging in metal-oxide-semiconductor field effect transistors. The introduction of atomic dopants (also referred to as "capping" layers) is an emerging approach to controllably modify ϕ_{eff}. Here, we investigate the energetic preference of the location of La, Y, Sc, Al, Ce, Ti, and Zr as atomic dopants within a model Pt/HfO_2/Si stack and the resulting variation of ϕ_{eff} using density functional theory calculations. Our results indicate that all the considered atomic dopants prefer to be situated at the interfaces. The dopant-induced variation of ϕ_{eff} is found to be strongly correlated to the dopant electronegativity and location. Dopants at the metal/HfO_2 interface decrease ϕ_{eff} with increasing dopant electronegativity, while a contrary trend is seen for dopants at the Si/HfO_2 interface. These results are consistent with available experimental data for La, Al, and Ti doping. Our findings, especially the identified correlations, have important implications for the further optimization and "scaling down" of transistors. © *2013 AIP Publishing LLC*. [http://dx.doi.org/10.1063/1.4821797]

I. INTRODUCTION

Metal/oxide interfaces have important technological applications, such as in electronics, catalysis, and thermal barrier coatings.[1–7] For any of these applications, precise control of the interfacial structure and chemistry towards good electrical, optical, magnetic, or mechanical properties is crucial. One notable example where metal/oxide interfaces are particularly relevant is the emerging "high-k" nanoelectronics device. The continuous size downscaling of complementary metal-oxide-semiconductor (CMOS) transistors has led to the replacement of SiO_2 with a HfO_2-based high dielectric constant (or high-k) oxide, and the polysilicon electrode with a metal gate. The desired metal electrodes need to display appropriate work functions that aligns the metal Fermi level (E_F) with either the valence band maximum (E_v) or the conduction band minimum (E_c) of the underlying Si substrate. However, interfacial effects such as charge transfer, bond formation, defect accumulation, and dipoles make achieving such an alignment a challenge.[8,9] As schematically shown in Figs. 1(a) and 1(b), merely using a metal with an appropriate vacuum work function (ϕ) may not be sufficient as the factors mentioned above could lead to an *effective* work function (ϕ_{eff}) which may result in a misalignment of E_F with respect to the Si band edges.

It is thus the value of ϕ_{eff} that really matters in the choice of the metal electrode.[8,9] For high-k based MOSFETs, ϕ_{eff} of metals has been demonstrated to be strongly dependent on the processing conditions that the device is subjected to.[10–14] It has been reported that ϕ_{eff} of many metal electrodes shifts toward the middle of the Si band gap upon high temperature annealing, regardless of its vacuum work function.[15]

An emerging way to control the relative position of E_F (or alternatively, ϕ_{eff}) is through the introduction of an interfacial dopant or "capping" layer either at the Si/HfO_2 interface or at the metal/HfO_2 interface.[16] Note that the preferred location of the capping layers will be determined by energetic and kinetic factors, and placement at either locations can be used to manipulate the E_F position or the ϕ_{eff} value, by tailoring the interface dipole moments (see Figs. 1(c) and 1(d)). For example, inserting a capping layer with a dipole moment pointing from Si to dielectric at Si/HfO_2 interfaces or pointing from dielectric to metal at metal/HfO_2 interfaces moves the metal E_F towards the Si E_c, which is desirable for n-type MOSFETs (see Fig. 1). For p-type MOSFETs, an opposite interface dipole moment could be introduced to align the metal E_F to the Si E_v. For example, Al_2O_3 and La_2O_3 have been reported as effective capping layers for p- and n-type MOSFET applications, respectively, which have been attributed to the different electronegativities of Al (1.61 Pauling), La (1.1 Pauling), and Hf (1.3 Pauling).[17–20]

Recent density functional theory (DFT) computations have been devoted to understanding the impact of these capping layers at metal/HfO_2 and Si/HfO_2 interfaces on ϕ_{eff}. It has been found that Al atoms substituting for Hf in the dielectric near the TiN/HfO_2 interface could increase ϕ_{eff}, while Te substitution of Hf at the Mo/HfO_2 interface decreases ϕ_{eff}.[17,18] Compared to metal/HfO_2 interface, dopants at Si/HfO_2 interfaces have been studied more intensively.[19–21] By investigating a group of dopants with different electronegativities and valences, e.g., La, Sr, Al, Nb, and Ti, the variation of the band offset at Si/HfO_2 interfaces, and hence the alignment of the metal E_F with the band edges of Si, is found to strongly correlate with dopant electronegativity. In general, it was demonstrated that dopants with electronegativity smaller (or larger) than that of Hf at Si/HfO_2 interfaces tend to move the metal E_F closer to E_c (or E_v) of Si.

Although the electronegativity of capping layer atoms at Si/HfO_2 interfaces have been demonstrated to be critical in

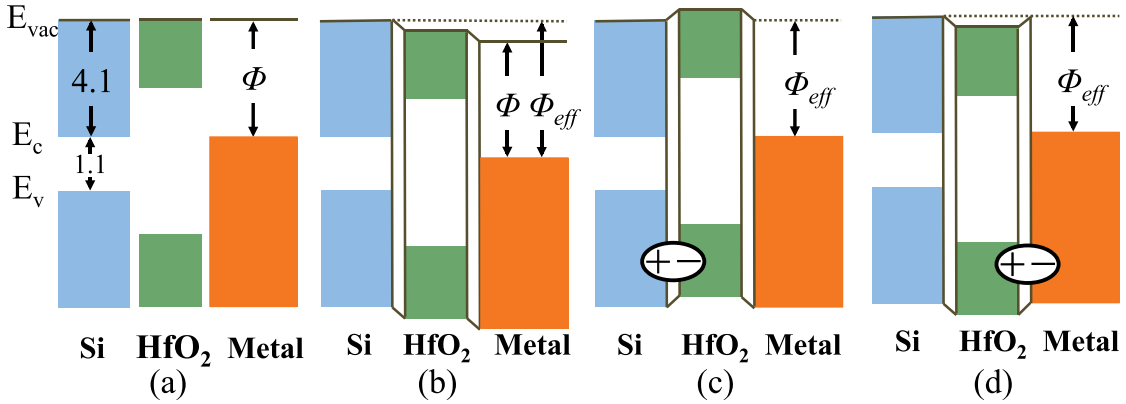

FIG. 1. Schematic of band alignment of HfO_2-based metal/oxide/silicon heterostructure for n-type MOSFETs. (a) Band structure before physical contact. The metal electrode is assumed to have the vacuum work function (ϕ) close to 4.1 eV such that the metal Fermi level aligns with Si conduction band minimum (E_c). (b) Due to Fermi level pinning, the Fermi level of metal electrode in physical contact with dielectrics is not aligned to the Si E_c, making the effective work function (ϕ_{eff}) different from ϕ. (c) Engineering the dipole moment at the Si/HfO_2 interface varies the metal Fermi level or ϕ_{eff} value. (d) Similar dipole moment engineering at metal/HfO_2 interface could also align the metal Fermi level to Si band edges. With the dipole moment pointed along the direction shown here, the metal Fermi level will be shifted towards the Si E_c, applicable for n-type MOSFETs.

determining ϕ_{eff}, a systematic understanding of the thermodynamic factors that control the preferred location of a large variety of capping layer atoms in the entire metal/HfO_2/Si stack and their impact on ϕ_{eff} is necessary for further targeted optimization of current as well as beyond-silicon and/or beyond-HfO_2 MOSFETs. In this work, we have adopted DFT calculations to explore a variety of dopants, namely, La, Y, Sc, Al, Ce, Ti, and Zr, within the whole Pt/HfO_2/Si stack. Our results indicate that atomic dopants are energetically more stable at the Pt/HfO_2 and the Si/HfO_2 interfaces. The variation of ϕ_{eff} upon the modulation of the interface chemistry through doping shows a strong correlation with the electronegativity as well as the position of the doping elements. These results, consistent with available experiments for La, Al, and Ti atomic doping, should assist in the engineering of metal/dielectric and semiconductor/dielectric interfaces to achieve desired band alignments.

II. METHODS AND MODELS

Our DFT calculations were performed using the VASP code[22] with the PW91 generalized gradient approximation[23] and a cut-off energy of 400 eV for the plane-wave expansion of the wave functions. Monkhorst-Pack k-point meshes of $5 \times 5 \times 5$ were used in the case of bulk monoclinic (m-) HfO_2, and diamond cubic Si, while the bulk face-centered cubic Pt requires $11 \times 11 \times 11$ meshes. The calculated lattice parameters are in good agreement with experiments. The computed a, b, and c lattice parameters of m-HfO_2 are 5.14, 5.19, and 5.3 Å, comparable with experimental values of 5.12, 5.17, and 5.29 Å.[24] The lattice parameters for Si and Pt are determined to be 5.46 and 3.98 Å, respectively, also in good agreement with the corresponding experimental values of 5.43 and 3.92 Å.[25,26]

To understand the energetics of dopants within the Pt/HfO_2/Si heterostructure, we have performed separate calculations for the Pt/HfO_2 interface, the HfO_2 slab, and the Si/HfO_2 interface. The (111) $(2 \times \sqrt{3})$ Pt and (001) (1×1) HfO_2 slabs were both stretched to match the (001) (1×1) Si slab. To some extent, this construction is expected to represent the situation where Si is the substrate. We do note that, in reality, although Si is the substrate (in single crystalline form), the HfO_2 layer is amorphous and the metal layer is polycrystalline. Nevertheless, our assumptions are expected to lead to conclusions and insights that are qualitatively correct. The Si/HfO_2 interface model is also assumed to contain a SiO_2 region (as shown in Fig. 2), considering the fact that the equilibrium phase at the Si/HfO_2 interface under standard processing conditions is silica-like.[27] The Pt/HfO_2 interface was assumed to contain a half monolayer of interfacial O atoms that passivates the HfO_2 slab.

The atomic dopants (X) have been considered to substitute a full monolayer of Hf atoms and form substitutional defects (X_{Hf}) at one of three locations: (1) at the Pt/HfO_2 interface, (2) at the Si/HfO_2 interface, and (3) in the interior "bulk" region of the HfO_2 slab. Various doping elements in

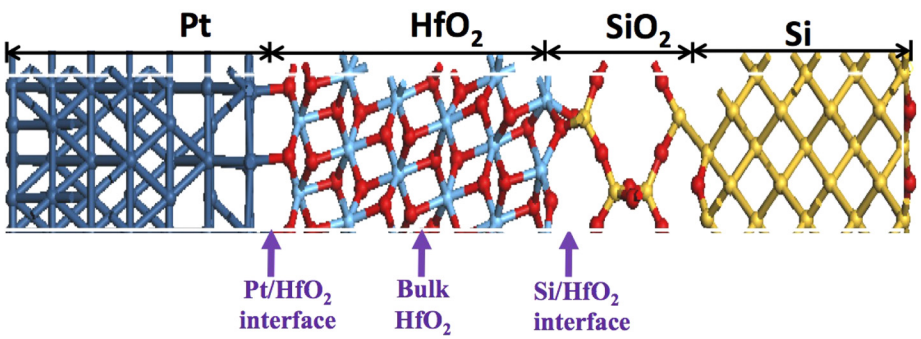

FIG. 2. Schematic of the Pt/HfO_2/Si heterostructure. The atomic dopants may substitute the Hf atom at the Pt/HfO_2 interface, within the bulk HfO_2 region or at the Si/HfO_2 interface, as indicated in the figure.

+3 and +4 valence states and with different electronegativities have been considered, namely, La, Al, Y, Sc, Ti, Ce, and Zr. For elements in the +3 valence state (namely, La, Al, Y, and Sc), substituting every 2 Hf atoms is accompanied by the removal of one O atom to maintain charge neutrality. For these dopants in +3 valence states, we have doubled the Pt/HfO_2, HfO_2, and Si/HfO_2 models along the *a* direction to explore several possible interfacial O configurations. Various configurations have been considered and we found the configuration with one O vacancy within each O monolayer on the hafnia side of the capping layer to be the most stable interface structure. The difference between ϕ_{eff} for the situations with and without the dopants (referred to as $\Delta\phi_{eff}$) was determined using the dipole moment change per interface area of the doped system with respect to the undoped ones (referred to as ΔD), using the following relationship: $\Delta\phi_{eff} = 4\pi\Delta D$.[28]

III. ENERGETICS OF ATOMIC DOPANTS WITHIN THE GATE STACK

Let us imagine that the doped heterostructure is formed by the following reaction:

$$Pt/HfO_2/Si + XO_n \Longleftrightarrow \text{doped-}Pt/HfO_2/Si + HfO_2. \quad (1)$$

The corresponding formation energy for the above reaction ($E_f = E_{doped} + E_{HfO_2} - E_{perfect} - E_{XO_n}$) describes the relative stability of the doped heterostructure with respect to the undoped case. E_{doped} and $E_{perfect}$ are the DFT energies of the doped and undoped heterostructures, respectively. E_{HfO_2} and E_{XO_n} are, respectively, the DFT energies of bulk *m*-HfO_2 and the most stable dopant oxide XO_n, with $n = 1.5$ or 2 depending on whether the valence state of X is +3 or +4.

The formation energies for doped heterostructure with respect to that of a perfect system are portrayed in Fig. 3. As we can see, most of the doping elements considered are energetically more favored at the interfaces. This indicates that substitutional dopants are likely to segregate to the interfaces, similar to what has been observed before for O (Hf) interstitials and vacancies.[29–32] To further investigate the tendency for dopants to segregate to the interfaces, we plot the formation energy difference between the doped heterostructure with dopants sitting at the interface and within the bulk HfO_2 region in Fig. 4, as a function of the dopant ionic size. For comparison, we note that the ionic size of Hf is almost identical to that of Zr. We find that the driving force for segregation toward interfaces is strongly related to the ionic radius of the doping elements. In general, increasing ionic radius favors the interfacial location for dopants. Moreover, compared to +4 valence state dopants, the interfacial segregation of doping elements with +3 valence state is more likely to occur, which is probably due to the large accompanying structural distortion. In fact, these dopant interfacial segregation tendencies are desirable from the point of view of effective tuning of the interface dipole moment, and consequently, the band alignment across heterostructures, which is discussed next.

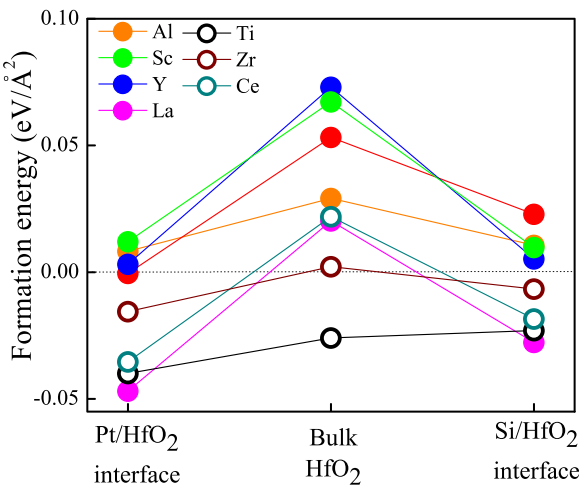

FIG. 3. Formation energy per interface area (in $eV/Å^2$) of doped-$Pt/HfO_2/Si$ heterostructures with respect to the undoped system, with X_{Hf} at the Pt/HfO_2 interface, in the bulk HfO_2 region, or at the Si/HfO_2 interface.

IV. MODULATION OF ϕ_{eff} DUE TO ATOMIC DOPANTS

As mentioned above, the change in ϕ_{eff} of Pt due to a dopant at a given location in the gate stack was determined by computation of the dopant-induced dipole moment change (ΔD) via the relation: $\Delta\phi_{eff} = 4\pi\Delta D$. The details of how *D* may be computed have been described elsewhere.[1,28] The variation of ϕ_{eff} due to the introduction of dopants at Pt/HfO_2 and Si/HfO_2 interfaces (i.e., $\Delta\phi_{eff}$) is captured in Fig. 5. We note that a dopant in the bulk part of HfO_2 does not contribute to a ϕ_{eff} change; i.e., $\Delta\phi_{eff} = 0$ in this case. For the cases when the dopant is at an interface, $\Delta\phi_{eff}$ is found to be strongly correlated with the electronegativity, as well as the position of the dopants. More specifically, when the dopants locate at metal/HfO_2 interfaces, $\Delta\phi_{eff}$ decreases with increasing of dopant electronegativity, while an opposite trend has been identified for dopants at Si/HfO_2

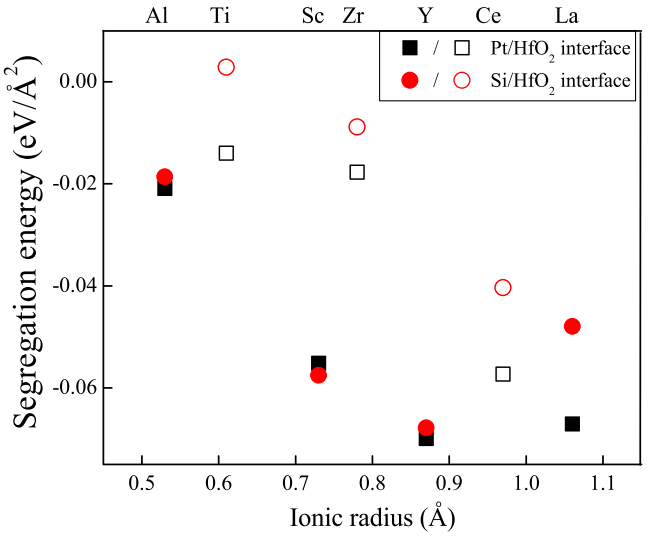

FIG. 4. Interfacial segregation energy per interface area (in $eV/Å^2$) of doped-$Pt/HfO_2/Si$ heterostructures as a function of dopant ionic radius. For comparison, we note that the ionic size of Hf is almost identical to that of Zr. The solid and open symbols stand for dopants with +3 and +4 valence states, respectively. The formation energy for dopants at Pt/HfO_2 and Si/HfO_2 interfaces are represented by squares and circles, respectively.

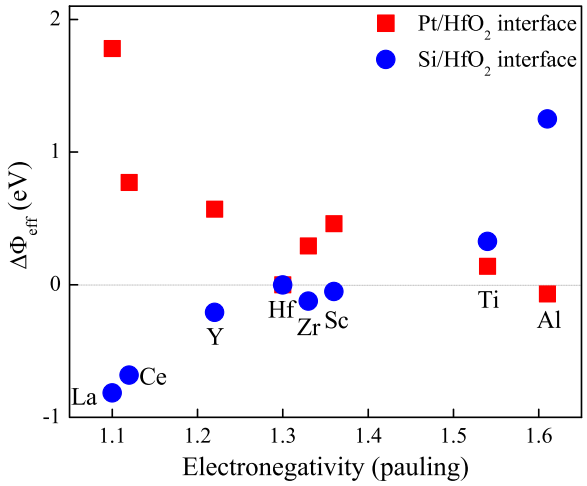

FIG. 5. Dopant induced changes in ϕ_{eff} (i.e., $\Delta\phi_{eff}$, in eV) as a function of the electronegativity of the doping elements.

interfaces. La and Al at Si/HfO_2 interfaces, which decrease and increase ϕ_{eff}, respectively, appear to be efficient dopants for *n*-type and *p*-type MOSFETs, consistent with prior experimental findings.[33] On the other hand, La at the Pt/HfO_2 interface increases ϕ_{eff}. This finding is also in agreement with the previous observations in which Pt deposited on HfLaO displays a larger ϕ_{eff} than that deposited on HfO_2.[34] On the other hand, we find Al at Pt/HfO_2 interfaces does not change ϕ_{eff} significantly. In fact, a similar phenomenon has been reported for as-deposited $TiSiN/HfO_2$ stacks with Al capping in which the diffusion of Al towards the Si/HfO_2 interface has not been triggered.[33] Recent studies on the impact of dopants on the threshold voltage shift of $Ru/HfO_2/Si$ gate stacks demonstrate that Ti at Ru/HfO_2 and Si/HfO_2 interfaces are most likely to increase ϕ_{eff} by 0.1 and 0.15 eV, respectively, which is also consistent with our predictions for Ti (Fig. 5).[35]

Finally, we note that Fig. 5 portrays a roughly linear relationship between the work function shift and the dopant electronegativity (with opposite slopes depending on the actual interfacial location of the dopant). Plots such as these (created for other more relevant gate stack systems, for example) are expected to provide design principles and guidelines for the proper choice of interfacial dopants.

V. SUMMARY

In sum, the energetics of La, Y, Sc, Al, Ce, Ti, and Zr dopants within the $Pt/HfO_2/Si$ stack, and the resulting variation of the metal effective work function have been investigated using density functional theory calculations. These calculations are intended to identify the specific role of dopant "capping" layers widely utilized in the emerging HfO_2-based transistor gate stacks. Our results indicate that dopants are more energetically favored at the interfaces, directly contributing to an interface dipole moment change. The variation of the metal effective work function is strongly correlated to the dopant electronegativity, as well as the interfacial position of the dopant. More specifically, dopants with small electronegativity (such as La) at Pt/HfO_2 and Si/HfO_2 interfaces will display a larger and smaller effective work function value, respectively. On the other hand, those with large electronegativity (e.g., Al) show an opposite trend. The close agreement of the obtained results with available experiments (e.g., for La, Al, and Ti doping) is indicative of the predictive capability of modern electronic structure calculations, which may be harnessed in the future design and engineering of heterostructure stacks.

ACKNOWLEDGMENTS

Financial support of this work through a grant from the National Science Foundation (NSF) and computational support through a NSF Teragrid Resource Allocation are gratefully acknowledged.

[1]H. Zhu, C. Tang, L. R. C. Fonseca, and R. Ramprasad, J. Mater. Sci. **47**, 7399 (2012).
[2]M. W. Finnis, J. Phys.: Condens. Matter **8**, 5811 (1996).
[3]J. I. Beltan and M. C. Munoz, Phys. Rev. B **78**, 245417 (2008).
[4]E. Saiz, R. M. Cannon, and A. P. Tomsia, Annu. Rev. Mater. Res. **38**, 197 (2008).
[5]Y. Jiang and J. R. Smith, J. Mater. Sci. **44**, 1734 (2009).
[6]S. Kulkova, A. Bakulin, S. Hocker, and S. Schmauder, IOP Conf. Ser: Mater. Sci. Eng. **38**, 012004 (2012).
[7]J. F. Bartolome, J. I. Beltran, C. F. Gutierrez-Gonzalez, C. Pecharroman, M. C. Munoz, and J. S. Moya, Acta Mater. **56**, 3358 (2008).
[8]J. Robertson, Rep. Prog. Phys. **69**, 327 (2006).
[9]J. Robertson, Solid-State Electron. **49**, 283 (2005).
[10]J. K. Schaeffer, L. R. C. Fonseca, S. B. Samavedam, Y. Liang, P. J. Tobin, and B. E. White, Appl. Phys. Lett. **85**, 1826 (2004).
[11]C.-H. Lu, G. M. T. Wong, M. D. Deal, W. Tsai, P. Majhi, C. O. Chui, M. R. Visokay, J. J. Chambers, L. Colombo, B. M. Clements, and Y. Nishi, IEEE Electron Device Lett. **26**(7), 445 (2005).
[12]D. Gu, S. K. Dey, and P. Majhi, Appl. Phys. Lett. **89**, 082907 (2006).
[13]H. Yang, Y. Son, S. Baek, and H. Hwang, Appl. Phys. Lett. **86**, 092107 (2005).
[14]M. T. Paffett, S. C. Gebhard, R. G. Windham, and B. E. Koel, J. Phys. Chem. **94**, 6831 (1990).
[15]H. Y. Yu *et al.*, IEEE Electron Device Lett. **25**, 337 (2004).
[16]S. Guha and V. Narayanan, Annu. Rev. Mater. Res. **39**, 181 (2009).
[17]K. Xiong *et al.*, J. Appl. Phys **104**, 074501 (2008).
[18]K. Xiong *et al.*, Appl. Phys. Lett. **92**, 113504 (2008).
[19]L. Lin *et al.*, J. Appl. Phys. **109**, 094502 (2011).
[20]X. Luo *et al.*, Phys. Rev. B **84**, 195309 (2011).
[21]A. G. Van Der Geest, P. Blaise, and N. Richard, Phys. Rev. B **86**, 085320 (2012).
[22]G. Kresse and J. Furthmuller, Phys. Rev. B **54**, 11169 (1996).
[23]J. P. Perdew *et al.*, Phys. Rev. B **46**, 6671 (1992).
[24]J. Adam and M. D. Rodgers, Acta Crystallogr. **12**, 951 (1959).
[25]C. R. Hubbard, H. E. Swanson, and F. A. Mauer, J. Appl. Crystallogr. **8**, 45 (1975).
[26]W. G. Ralph and Wyckoff, *The Structure of Crystals* (Reinhold, New York, 1935), p. 11.
[27]H. Zhu, C. Tang, and R. Ramprasad, Phys. Rev. B **82**, 235413 (2010).
[28]H. Zhu and R. Ramprasad, Phys. Rev. B **83**, 081416(R) (2011).
[29]C. Tang, B. Tuttle, and R. Ramprasad, Phys. Rev. B **76**, 073306 (2007).
[30]C. Tang and R. Ramprasad, Phys. Rev. B **75**, 241302 (2007).
[31]C. Tang and R. Ramprasad, Appl. Phys. Lett. **92**, 152911 (2008).
[32]C. Tang and R. Ramprasad, Appl. Phys. Lett. **92**, 182908 (2008).
[33]H. C. Wen, "Systematic evaluation of metal gate electrode effective work function and its influence on device performance in CMOS devices," Ph.D. dissertation (University of Texas, Austin, TX, 2006).
[34]X. P. Wang *et al.*, IEEE Electron Device Lett. **28**, 258 (2007).
[35]W. J. Maeng *et al.*, Appl. Phys. Lett. **96**, 082905 (2010).